NANO LETTERS

2002
Vol. 2, No. 8
823−826

Diameter-Dependent Combination Modes in Individual Single-Walled Carbon Nanotubes

Jialong Zhao,[†] Chaoyang Jiang,[†] Yuwei Fan,[‡] Marko Burghard,[‡] Thomas Basché,[†] and Alf Mews*,[†]

Institut für Physikalische Chemie, Universität Mainz, Mainz D-55099, Germany, and Max-Planck-Institut für Festkörperforschung, Heisenbergstrasse 1, Stuttgart D-70569, Germany

Received April 9, 2002; Revised Manuscript Received May 22, 2002

ABSTRACT

Resonant Raman spectra of individual single-walled carbon nanotubes (SWNTs) and thin SWNT bundles have been acquired by scanning confocal Raman microscopy. The position of several Raman modes was followed in dependence of the diameter-dependent radial-breathing modes (RBMs) and the excitation energy. For semiconducting nanotubes a systematic shift of one of the bands between 1650 and 2100 cm^{-1} is observed with decreasing nanotube diameter and attributed to a combination mode of the G-band and the RBM.

Since their discovery by Iijima and Ichibashi in 1993,[1] single-walled carbon nanotubes (SWNTs) have received considerable attention in the fields of fundamental research and technological applications.[2,3] This is mainly due to the fact that SWNTs are molecular wires that can be either metallic or semiconducting, depending on their symmetry and diameter. Raman spectroscopy has proven to be a sensitive tool for studying the vibrational and electronic properties of carbon nanotubes.[4] For example the frequency of the radial breathing mode (RBM) in the region of 100−350 cm^{-1} is found to be inversely proportional to the diameter of the nanotube.[4−8] Moreover, the shape of the so-called G-band between 1500 and 1600 cm^{-1} allows to distinguish between semiconducting and metallic nanotubes. The metallic nanotubes exhibit an additional band at about 1550 cm^{-1}, which originates from the coupling of the electronic continuum to the tangential atomic vibrations, and can be fitted with a Breit−Wigner−Fano (BWF) line shape.[9−11]

In the frequency range between 1650 and 2100 cm^{-1}, two additional weak Raman bands can be observed in SWNTs.[12−16] The spectral positions of these bands shift upon excitation with different laser frequencies. Since this could be due to selective excitation of nanotubes of different diameter, these modes were tentatively explained as the combination modes $\omega_G + \omega_{RBM}$ and $\omega_G + 2\omega_{RBM}$ of the RBM and the G-band.[12−14] On the other hand, Raman bands in the same frequency range could also be observed in highly oriented pyrolytic graphite (HOPG) and graphite whiskers, and were explained by combination modes of the G-line and acoustic phonons.[17]

A detailed study of the origin of these bands in SWNT ensembles is difficult because bulk SWNT samples usually exhibit a broad variation of nanotube diameters and hence a broad distribution of RBMs and possible combination modes. The spectral selection using different excitation energies, on the other hand, might not only resonantly enhance Raman scattering of nanotubes within a certain diameter range, but is also sensitive to the phonon dispersive behavior of SWNTs.[18]

To overcome the problem of ensemble averaging, the method of Raman microscopy has been introduced where isolated bundles and even single SWNTs can be investigated individually.[15,19] With this method it was even possible to determine the (n,m) indices of the chiral vector of isolated nanotubes by the anti-Stokes/Stokes resonant Raman intensity ratio of the RBM.[20,21]

In this paper, we combine spatial and frequency selection. We used scanning confocal Raman microscopy together with atomic force microscopy (AFM) to overcome sample averaging by investigating isolated SWNTs and thin SWNT bundles which show only one single RBM. In addition, we used two different laser wavelengths to selectively excite semiconducting or metallic nanotubes and also to determine the effect of different excitation energy upon the investigated Raman bands.

The SWNTs produced by the arc discharge method were purchased from Carbolex (Lexington, USA). The nanotubes

* Corresponding author. E-mail: alf.mews@uni-mainz.de.
[†] Universität Mainz.
[‡] Max-Planck-Institut für Festkörperforschung.

10.1021/nl025576w CCC: $22.00
Published on Web 06/06/2002

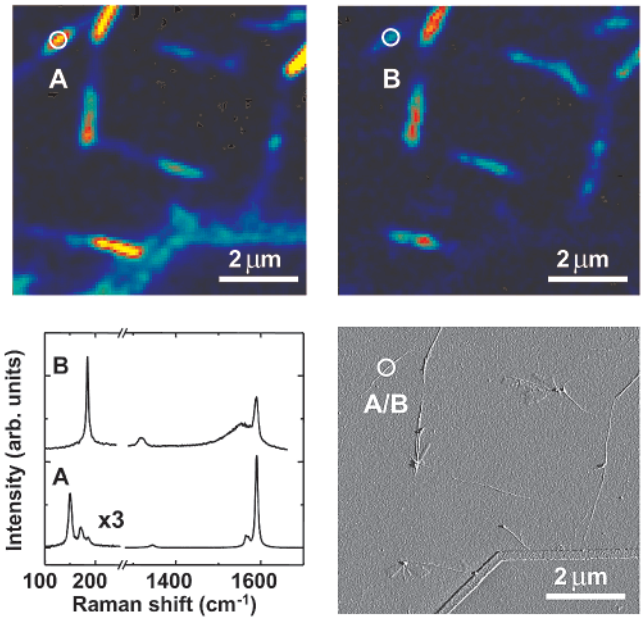

Figure 1. Spatial and frequency selection of carbon nanotubes. Raman images (a), (b) and Raman spectra A, B were acquired under excitation wavelengths of 514.5 and 647.1 nm, respectively. Therefore the Raman spectra A and B in (c) correspond to the scattering from semiconducting and metallic nanotubes within the same SWNT bundle (thickness ~ 2.7 nm) marked in the corresponding AFM image (d).

were deposited on a chemically modified Si_3N_4 membrane with gold markers to address the same SWNTs in the Raman- and atomic force microscope. Confocal Raman images and spectra were acquired at room temperature using Ar−Kr laser lines of 514.5 nm (2.41 eV) or 647.1 nm (1.92 eV). An inverted Zeiss microscope equipped with a piezo scanner and a high numerical aperture microscope objective (100×, NA = 0.9) was used for addressing different SWNTs. Typically 1 mW of circularly polarized light was focused down to a diffraction-limited spot size (fwhm <500 nm), resulting in an excitation power of the order of 800 kW/cm^2 in the center of the spot. To record an image, the sample was raster scanned through the excitation spot, and the G-line of the Raman light was detected in back reflection with an avalanche photodiode. The spectra were taken with a liquid nitrogen cooled charge-coupled device (CCD) behind a 500 mm single grating spectrograph. The spectral resolutions of the Raman systems for 300 and 1800 grooves/mm gratings are about 8 and 1.5 cm^{-1}, respectively.

Figures 1a and b show two typical Raman images of the same sample area that were acquired using excitation wavelengths of 514.5 (a) and 647.1 nm (b), respectively. The spectra A/B in Figure 1c were also taken with different excitation energies and result from the same bundle as marked in the corresponding AFM picture in Figure 1d. Due to selective resonant enhancement,[7,22] the Raman image in Figure 1a originates mainly from the semiconducting nanotubes, because the laser energy is in resonance with the electronic transition energy E_{44}^S for nanotubes in the diameter range between 1.9 and 1.5 nm and with E_{33}^S for nanotubes between 1.5 and 1.2 nm.[7] The diameter distribution of the carbon nanotubes used in this experiment was estimated to be 1.47 ± 0.25 nm based on the relation: $\omega_{RBM} = 248\ \text{cm}^{-1}/d\ (\text{nm})$.[7] For example the Raman spectrum A in Figure 1c was taken from a bundle with a height of 2.7 nm as judged from the corresponding AFM profile. This spectrum shows three resolved RBMs consistent with at least three different semiconducting nanotubes within the bundle.

Figure 1b shows a Raman image of the identical sample area but acquired with an excitation wavelength of 647.1 nm. This image results mainly from metallic nanotubes because the excitation energy (1.92 eV) is in resonance with the electronic transition E_{11}^M for metallic nanotubes between 1.2 and 1.4 nm. On the other hand, this energy is also in resonance with the transition E_{33}^S of relatively thick semiconducting nanotubes between 1.6 and 1.8 nm, which would show an RBM frequency $\omega_{RBM} = 155-138\ \text{cm}^{-1}$. However, the spectrum B in Figure 1c, which was taken at the same position as A, shows a single RBM frequency of 184 cm^{-1}, consistent with a resonantly excited metallic tube within the same bundle. The appearance of the broad BWF line centered at 1556 cm^{-1} further supports this assignment.[9−11]

This example shows that it is possible to perform selective Raman spectroscopy of metallic and semiconducting nanotubes within thin bundles of SWNTs. To reliably study the diameter-dependent combination modes of the G-line and the RBM, only those thin nanotube bundles which exhibit single RBM lines were further investigated. In principle, intertube interaction within a given bundle could shift the RBM frequency by up to 10 cm^{-1}.[8] However, this would alter only the diameter distribution as determined from the RBMs but not the coupling between the G-band and the measured RBMs as discussed below.

Figures 2 and 3 show Raman spectra of SWNTs excited with laser wavelengths of 647.1 and 514.5 nm, respectively. All of these spectra exhibit a single narrow RBM in the range of 140 to 200 cm^{-1}, the D-band at ~1343 cm^{-1}, and the G-band around ~1590 cm^{-1}. The measured line width are between 3 and 12 cm^{-1} for the RBM and 6−12 cm^{-1} for the sharp component of the G-band at 1590 cm^{-1}, which is consistent with Raman measurements on individual tubes as has recently been shown.[23]

Spectrum A in Figure 2 (λ_{ex} = 647.1 nm) was recorded from a SWNT which was only 1.5 nm in height and might therefore result from a single nanotube. The Raman spectrum however does not show the characteristic BWF line at the low-frequency side of the G-line, even though the excitation energy was 1.92 eV. Since the RBM frequency (154 cm^{-1}) is consistent with a tube diameter of 1.6 nm, we assume that this particular tube is semiconducting. The Raman spectra (B−D), however, can be associated with resonantly excited metallic SWNTs that show the BWF line, the relative intensity of which is dependent on the bundle thickness.[24] The enlarged spectra in the frequency range between 1700 and 2200 cm^{-1} show the additional weak phonon modes P1 and P2, which peak at about 1750 and 1940 cm^{-1}. These modes were tentatively assigned to the combination modes $\omega_G + \omega_{RBM}$ and $\omega_G + 2\omega_{RBM}$ between the RBM and the G-band.[12−14] However, it can be seen that these bands do

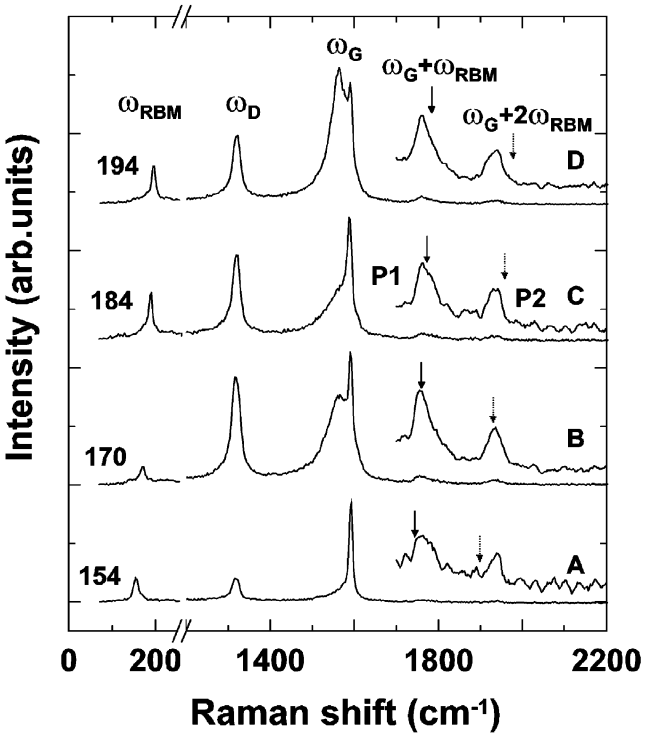

Figure 2. Raman spectra recorded using an excitation energy of 1.92 eV. The spectra A to D represent different SWNTs with the RBM frequencies of 154, 170, 184, and 194 cm^{-1} and with the bundle thicknesses of 1.5, 4.1, 2.7, and 3.9 nm, respectively. On the left-hand side of each spectrum, the RBM frequencies are shown. The combination modes $\omega_G + \omega_{RBM}$ and $\omega_G + 2\omega_{RBM}$ should appear at the positions labeled by vertical arrows.

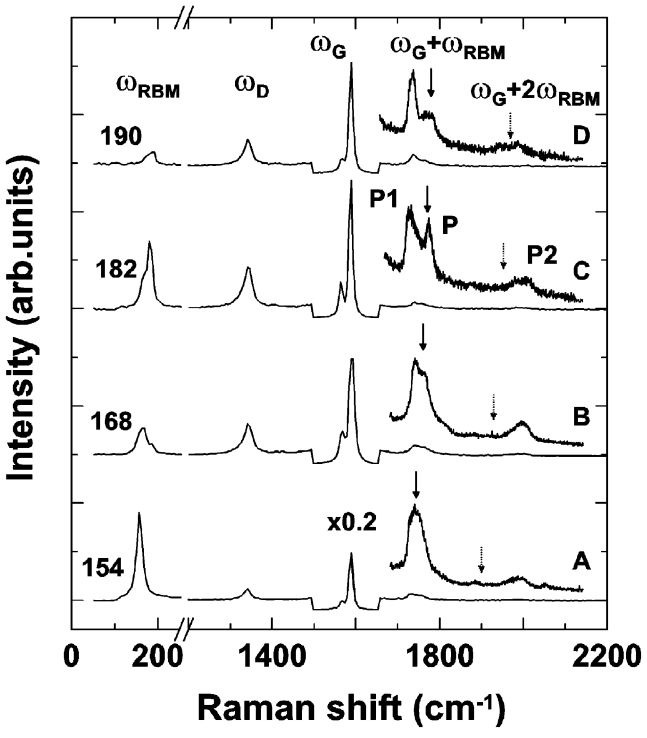

Figure 3. Raman spectra of thin nanotube bundles recorded with the excitation energy of 2.41 eV. The spectra A to D correspond to different SWNTs with the RBM frequencies of 154, 170, 182, and 190 cm^{-1} and with the bundle thicknesses of 3.2, 5.0, 2.8, and 3.9 nm, respectively. The vertical arrows mark the positions of the combination modes $\omega_G + \omega_{RBM}$ and $\omega_G + 2\omega_{RBM}$, respectively.

not show a systematic shift similar to the respective RBM frequency, which is a first indication that the bands P1 and P2 are not combination modes as suggested before.

Figure 3 ($\lambda_{ex} = 514.5$ nm) shows Raman spectra of several individual SWNTs and thin SWNT bundles acquired with a respective excitation energy of 2.41 eV, which again show only a single RBM. All of those spectra do not show the BWF line, which is characteristic for metallic tubes, and are attributed to semiconducting SWNTs. The enlarged part shows again two distinguishable phonon bands P1 and P2 which are now shifted to about 1740 and 1990 cm^{-1}, respectively. Again, no systematic shift of these bands can be seen for different tube diameters. On the other hand, a third band denoted as P clearly evolves from P1. The position of this band clearly follows the expected frequency evolution for $\omega_G + \omega_{RBM}$, as marked by the vertical arrows. Therefore, we attribute this band to the combination mode of the G-line and the RBM.

The results are summarized in Figure 4 where the peak positions of the phonon bands between 1650 and 2100 cm^{-1} are plotted as a function of the inverse nanotube diameter for both excitation energies. It can clearly be seen that phonon modes P1 and P2 do not show a systematic dependence on the nanotube diameter, which would be expected if these bands were combination modes of the G-line and the RBM as predicted before.[12−14] The expected frequency for the combination mode of the G-line and the RBM is shown by the solid line in Figure 4, which displays

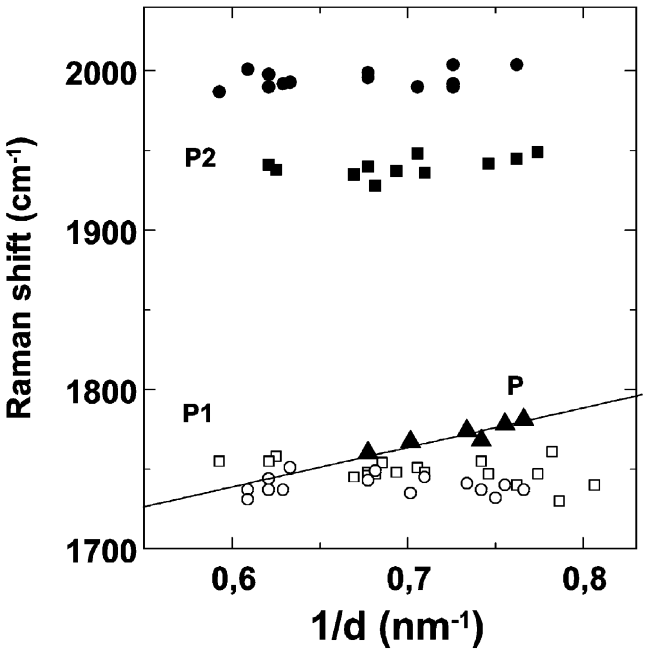

Figure 4. Phonon modes P (triangles), P1 (hollow symbols), and P2 (solid symbols) excited with 647.1 nm (squares) and 514.5 nm (circles) at different inverse nanotube diameters, as determined from the RBM frequency. The solid line shows the expected frequency of the combination modes as calculated with the relation $\omega_C = \omega_G + \omega_{RBM}$.

the relation $\omega_C = \omega_G + \omega_{RBM}$ for a value of $\omega_G = 1590$ cm^{-1}. Obviously the solid triangles which represent the

position of the resolved combination modes P of the semiconducting nanotubes follow this dependence.

In general, the Raman signal is not only enhanced by resonance conditions with the incident but also with the scattered photon. However, only the resonance condition with the incident light will enhance all Raman signals of a given SWNT[23] and hence contribute to the combination mode. Therefore the combination mode of the semiconducting SWNTs was always observed at the sum frequency $\omega_G + \omega_{RBM}$, as can be seen from Figure 3. On the other hand, the diameter-dependent combination modes could not be directly observed in the Raman spectra of the metallic nanotubes. Based on the RBM, the combination mode should appear near the phonon mode P1 of the metallic nanotubes and could possibly not be resolved.

The origin of the phonon modes P1 and P2 is not clear at present and should be subject of further theoretical investigations. It is noted that at least the phonon mode P2 changes with excitation energy. This "dispersive behavior" could already be seen, for example, for the D-band in graphite, and was explained by double resonant Raman processes.[25,26] Furthermore, the energies of phonon modes P1 and P2 are slightly different from one bundle to another, which might be due to different intra bundle interactions. The difference could also result from different chiralities of the nanotubes, as it has been recently theoretically predicted that, for example, the D-band frequency in SWNTs depends not only on the tube diameter but also on their (n,m) indices.[26−28]

In summary, the combination mode between the G-line and the RBM has been identified in isolated SWNTs and small bundles by confocal Raman microscopy in combination with AFM. The diameter-dependent combination mode was clearly observed in the semiconducting nanotubes but not in the metallic nanotubes. The phonon modes P1 and P2, which had been assigned to be combinations modes so far, did not show a systematic dependence on the tube diameter and need to be reassigned in the future.

Acknowledgment. One of the authors (J.Z.) would like to thank Dr. Zhonghua Yu for valuable discussions. We also thank Dr. Guenther Philipp for providing the substrates. This work was supported by the BMBF under contract No. 03C0302B9.

References

(1) Iijima, S.; Ichibashi, T. *Nature* **1993**, *363*, 603.
(2) Saito, R.; Dresselhaus, G.; Dresselhaus, M. S. *Physical Properties of Carbon Nanotubes*; Imperial College Press: London, 1998.
(3) Dresselhaus, M. S.; Eklund, P. C. *Adv. Phys.* **2000**, *49*, 705.
(4) Rao, A. M.; Richter, E.; Bandow, S.; Chase, B.; Eklund, P. C.; Williams, K. A.; Fang, S.; Subbaswamy, K. R.; Menon, M.; Thess, A.; Smalley, R. E.; Dresselhaus, G.; Dresselhaus, M. S. *Science* **1997**, *275*, 187.
(5) Bandow, S.; Asaka, S.; Saito, Y.; Rao, A. M.; Grigorian, L.; Richter, E.; Eklund, P. C. *Phys. Rev. Lett.* **1998**, *80*, 3779.
(6) Milnera, M.; Kürti, J.; Hulman, M.; Kuzmany, H. *Phys. Rev. Lett.* **2000**, *84*, 1324.
(7) Jorio, A.; Saito, R.; Hafner, J. H.; Lieber, C. M.; Hunter, M.; McClure, T.; Dresselhaus, G.; Dresselhaus, M. S. *Phys. Rev. Lett.* **2001**, *86*, 1118.
(8) Rao, A. M.; Chen, J.; Richter, E.; Schlecht, U.; Eklund, P. C.; Haddon, R. C.; Venkateswaran, U. D.; Kwon, Y. K.; Tománek, D. *Phys. Rev. Lett.* **2001**, *86*, 3895.
(9) Pimenta, M. A.; Marucci, A.; Empedocles, S. A.; Bawendi, M. G.; Hanlon, E. B.; Rao, A. M.; Eklund, P. C.; Smalley, R. E.; Dresselhaus, G.; Dresselhaus, M. S. *Phys. Rev. B* **1998**, *58*, 16016.
(10) Kataura, H.; Kumazawa, Y.; Maniwa, Y.; Umezu, I.; Suzuki, S.; Ohtsuka, Y.; Achiba, Y. *Synth. Met.* **1999**, *103*, 2555.
(11) Brown, S. D. M.; Jorio, A.; Corio, P.; Dresselhaus, M. S.; Dresselhaus, G.; Saito, R.; Kneipp, K. *Phys. Rev. B* **2001**, *63*, 155414.
(12) Brown, S. D. M.; Corio, P.; Marucci, A.; Pimenta, M. A.; Dresselhaus, M. S.; Dresselhaus, G. *Phys. Rev. B* **2000**, *61*, 7734.
(13) Corio, P.; Brown, S. D. M.; Marucci, A.; Pimenta, M. A.; Kneipp, K.; Dresselhaus, G.; Dresselhaus, M. S. *Phys. Rev. B* **2000**, *61*, 13202.
(14) Brown, S. D. M.; Corio, P.; Marucci, A.; Dresselhaus, M. S.; Pimenta, M. A.; Kneipp, K. *Phys. Rev. B* **2000**, *61*, 5137.
(15) Mews, A.; Koberling, F.; Basché, T.; Philipp, G.; Duesberg, G. S.; Roth, S.; Burghard, M. *Adv. Mater.* **2000**, *12*, 1210.
(16) Tan, P.; Tang, Y.; Deng, Y.; Li, F.; Wei, Y.; Cheng, H. *Appl. Phys. Lett.* **1999**, *75*, 1524.
(17) Tan, P.; Hu, C.; Dong, J.; Shen, W.; Zhang, B. *Phys. Rev. B* **2001**, *64*, 214301.
(18) Saito, R.; Jorio, A.; Souza Filho, A. G.; Dresselhaus, G.; Dresselhaus, M. S.; Pimenta, M. A. *Phys. Rev. Lett.* **2002**, *88*, 027401.
(19) Yu, Z.; Brus L. E. *J. Phys. Chem. B* **2001**, *105*, 1123.
(20) Souza Filho, A. G.; Jorio, A.; Hafner, J. H.; Lieber, C. M.; Saito, R.; Pimenta, M. A.; Dresselhaus, G.; Dresselhaus, M. S. *Phys. Rev. B* **2001**, *63*, 241404.
(21) Yu, Z.; Brus, L. E. *J. Phys. Chem. B* **2001**, *105*, 6831.
(22) Saito, R.; Dresselhaus, G.; Dresselhaus, M. S. *Phys. Rev. B* **2000**, *61*, 2981.
(23) Jorio, A.; Souza Filho, A. G.; Dresselhaus, G.; Dresselhaus M. S.; Swan, A. K.; Ünlü, M. S.; Goldberg, B. B.; Pimenta, M. A., Hafner, J. H.; Lieber, C. M.; Saito, R. *Phys. Rev. B* **2002**, *65*, 155412.
(24) Jiang, C.; Kempa, K.; Zhao, J.; Schlecht, U.; Kolb, U.; Basché, T.; Burghard, M.; Mews, A., submitted.
(25) Thomsen, C.; Reich, S. *Phys. Rev. Lett.* **2000**, *85*, 5214.
(26) Maultzsch, J.; Reich, S.; Thomsen, C. *Phys. Rev. B* **2001**, *64*, 121407.
(27) Pimenta, M. A.; Jorio, A.; Brown, S. D. M.; Souza Filho, A. G.; Dresselhaus, G.; Hafner, J. H.; Lieber, C. M.; Saito, R.; Dresselhaus, M. S. *Phys. Rev. B* **2001**, *64*, 041401.
(28) Souza Filho, A. G.; Jorio, A.; Dresselhaus, G.; Dresselhaus, M. S.; Saito, R.; Swan, A. K.; Ünlü, M. S.; Goldberg, B. B.; Hafner, J. H.; Lieber, C. M.; Pimenta, M. A. *Phys. Rev. B* **2002**, *65*, 035404.

NL025576W